16TH EUROPEAN CONFERENCE ON EARTHQUAKE ENGINEERING THESSALONIKI 18 - 21 JUNE 2018

DESIGN METHOD FOR PIPELINES TO WITHSTAND LONGITUDINAL SLOPE MOVEMENT

Nobuhisa SUZUKI[1], Takekazu ARAKAWA[2]

ABSTRACT

This paper describes a simple design method to calculate the longitudinal inelastic strain distribution induced in a pipeline by longitudinal slope movement. Three solutions are derived assuming an elastic and unpressurized pipeline and elastic-perfect plastic bilinear soil springs. Solution-1 is provided to calculate the elastic strain distribution when the soil springs behave elastically, which is the displacement controlled condition. Solution-2 is used to obtain the elastic strain distribution in cases where some parts of the soil springs yield, which is the partially load controlled condition. Solution-3 gives the elastic strain distribution in the case where almost all the soil springs yield. Each elastic strain distribution is converted to the inelastic strain distribution through a strain conversion procedure where the longitudinal tensile properties and the constraint that the pipe strain does not exceed the ground strain are taken into account. The key parameter in the strain conversion procedure is the pivot strain, which is defined by the profile of the slope movement, the pipe-soil interaction parameters, and the soil spring parameters. When a pipeline is pressurized, the effects on the longitudinal tensile properties must be considered in the strain conversion procedure.

Keywords: Pipeline; Seismic design; Slope movement; Strain conversion, Pivot strain.

1. INTRODUCTION

A detailed study of pipeline design is required to ensure seismic integrity against permanent ground deformation (PGD) generated along a slope (Suzuki and Nakane 1989; Suzuki 1995). The Japan Gas Association (JGA) published strain-based seismic design guidelines for pipelines to withstand PGD (JGA 2001 and 2016), in which regression formulas are presented based on results obtained by finite element analyses. Other seismic design guidelines for withstanding temporary ground deformation (TGD) (JGA 1983; 2001 and 2004) describe design formulas including parameters with respect to the profile of TGD. However, the design formulas are independent of the tensile properties of the pipeline. Therefore, this paper describes a simple design method to calculate the inelastic strain distribution of a pipeline subjected to axial deformation induced by slope movement considering the stress-strain relationship. The design formulas of Solution-1 were derived to estimate the displacement controlled elastic deformation of a pipeline generated by PGD with small ground displacement assuming an unpressurized elastic pipe and elastic soil springs. The other design formulas of Solution-2 and Solution-3 were derived to calculate the load controlled elastic deformation of a pipeline generated by PGD with large ground deformation assuming an unpressurized elastic pipe and bilinear soil springs.

The inelastic strain distribution of an unpressurized pipeline is calculated through a strain conversion procedure using the obtained elastic strain distribution. The strain conversion procedure requires the longitudinal tensile properties of the pipe obtained by tensile tests using rectangular test specimens. The inelastic pipe strain is obtained at the point where the stress-strain curve intersects a line segment defined by the elastic solution and the pivot strain. The pivot strain is the key parameter in the proposed strain conversion procedure. In cases where a pipeline is pressurized, the inelastic strain

[1]Consultant, JFE Steel Corporation, Tokyo, Japan, bell-wood@muh.biglobe.ne.jp
[2]Senior Staff General Manager, JFE Steel Corporation, Tokyo, Japan, t-arakawa@jfe-steel.co.jp

distribution is calculated by using the elastic strain distribution and tensile properties considering the effect of pressure.
Validation of Solution-1, Solution-2, and Solution-3 was conducted by comparing results obtained by finite element analyses (FEA). An X65, 24” unpressurized or pressurized pipeline was used for the validation. As the result of this validation, the elastic strain distributions of the pipeline estimated by the solutions coincided closely with the results obtained by FEA assuming elastic deformation of the pipeline. The inelastic strain distributions predicted through the strain conversion procedure also showed excellent agreement with the results of FEA incorporating inelastic deformation of the pipeline.

2. ASSUMPTIONS TO SOLVE LONGITUDINAL DEFORMATION OF PIPELINE

2.1 Longitudinal Slope Movement and Ground Strain

The longitudinal slope movement along a pipeline is illustrated on the left side in Figure 1, and the displacements are represented as Equation 1. The longitudinal strain distribution generated in the ground is shown on the right side in Figure 1 and is represented as Equation 2. The maximum compressive strain of the ground appears at $x=L/4$, as represented in Equation 3. The maximum tensile strain is found at $x=-L/4$ and is expressed as Equation 4. This kind of slope movement can be observed in liquefied areas or mountainous areas (Suzuki 1989; 1995 and 2014).

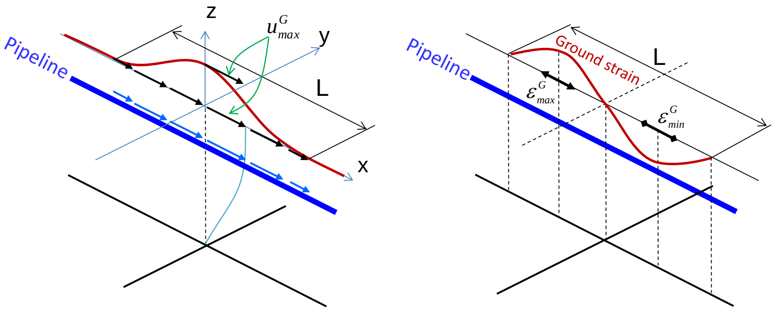

Figure 1. Longitudinal displacement (left) and longitudinal strain distribution (right) of ground caused by longitudinal slope movement

$$u^G(x)=\left\{1+cos\left(\frac{2\pi}{L}x\right)\right\}\frac{u^G_{max}}{2} \tag{1}$$

$$\varepsilon^G(x)=-\frac{\pi}{L}u^G_{max}\,sin\left(\frac{2\pi}{L}x\right) \tag{2}$$

$$\varepsilon^G_{min}=\varepsilon^G\left(\frac{L}{4}\right)=-\frac{\pi}{L}u^G_{max} \tag{3}$$

$$\varepsilon^G_{max}=\varepsilon^G\left(-\frac{L}{4}\right)=\frac{\pi}{L}u^G_{max} \tag{4}$$

Where, u^G_{max} is a maximum ground displacement, L is a wavelength, and $u^G(x)$ and $\varepsilon^G(x)$ represent the displacement and strain distributions of the ground in the longitudinal direction, respectively. In addition, ε^G_{min} means the maximum compressive strain and ε^G_{max} is the maximum tensile strain.

2.2 Geometry and Tensile Properties of Pipeline

It is assumed that a pipeline having an infinite length is laid downward along a slope, as illustrated in

Figure 1. It is also assumed that the pipeline is elastic and unpressurized and has uniform dimensions. In addition, the burial depth of the pipeline is constant and the surrounding soils have uniform soil spring properties.

2.3 Pipe-Soil Interaction in Longitudinal Direction

The longitudinal soil spring properties are idealized by the elastic and perfect-plastic model represented in Figure 2 (JGA 1983, ASCE 1984).

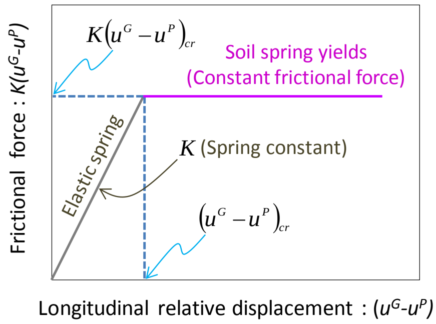

Figure 2. Soil spring properties in longitudinal direction

Herein, u^G and u^P mean the longitudinal displacement of the ground and pipeline, respectively. And K expresses the elastic soil spring constant in the longitudinal direction, and $u^G{}_{cr}$ represents the critical displacement of the elastic soil spring. Moreover, the soil spring yields when the relative displacement $(u^G\text{-}u^P)$ exceeds $(u^G\text{-}u^P)_{cr}$, and the soil spring achieves a constant frictional force $K(u^G\text{-}u^P)_{cr}$ loaded on the pipeline in the longitudinal direction.

3. LONGITUDINAL DEFORMATION OF UNPRESSURIZED ELASTIC PIPELINE

3.1 Solution-1: Deformation of Elastic Pipeline Supported by Elastic Soil Springs

The differential equation representing the longitudinal deformation of an elastic and unpressurized pipeline is expressed as Equation 5 (Kuesel 1969, JGA 1983, ASCE 1984).

$$\frac{d^2u^{PE}(x)}{dx^2} = -\alpha^2\left(u^G(x)-u^{PE}(x)\right) \tag{5}$$

Where, $u^{PE}(x)$ and $u^G(x)$ represent the longitudinal deformations of an elastic pipe and the ground, respectively. E means Young's modulus, A expresses the section area of the pipe, and K is the elastic soil spring constant per unit length of the pipe. In addition, α is the pipe-soil interaction parameter in the longitudinal direction and is represented as $\alpha=(K/EA)^{1/2}$, and EA means the axial rigidity. The elastic spring constant K is expressed as $K=\pi Dk$, where D and k are the pipe diameter and the elastic soil spring constant per unit area, respectively.

As long as the soil springs behave elastically, Equation 6 is satisfied spontaneously at $x=0$, the origin of the coordinate. Inserting the ground displacement expressed as Equation 1 into Equation 5, the stress and strain of the pipeline are obtained as Equations 7 and 8, respectively, in terms of the conversion factor F_s, as represented in Equation 9. Equation 10 was obtained considering Equation 6, which distinguishes the displacement controlled condition from the load controlled condition. Equation 10 was transformed into Equation 11, which is useful to calculate the maximum ground displacement less than that when the soil springs behave elastically.

$$u^G(0)-u^{PE}(0)\leq u^G_{cr} \tag{6}$$

$$u^{EP}(x)=\left[1+F_s\left\{\cos\left(\frac{2\pi}{L}x\right)-\left(\frac{2\pi}{L}\right)^2 e^{-\alpha L/2}\cosh(\alpha x)\right\}\right]\frac{u^G_{max}}{2} \qquad \left(-\frac{L}{2}\le x\le\frac{L}{2}\right) \tag{7}$$

$$\varepsilon^{PE}(x)=-F_s\left\{\sin\left(\frac{2\pi}{L}x\right)+\frac{2\pi}{\alpha L}e^{-\alpha L/2}\sinh(\alpha x)\right\}\frac{\pi}{L}u^G_{max} \qquad \left(-\frac{L}{2}\le x\le\frac{L}{2}\right) \tag{8}$$

$$F_s=\frac{1}{1+(2\pi/\alpha L)^2} \tag{9}$$

$$\left\{\left(1+e^{-\alpha L/2}\right)\frac{u^G_{max}}{2u^G_{cr}}-1\right\}^{1/2}\le\frac{\alpha L}{2\pi} \tag{10}$$

$$u^G_{max}\le u^G_{elastic}=\frac{2u^G_{cr}}{(1-F_S)\left(1+e^{-\alpha L/2}\right)} \tag{11}$$

Where, $u^{PE}(x)$ *and* $\varepsilon^{PE}(x)$ represent the longitudinal stress and strain distributions of the elastic pipe, respectively, and F_s is a conversion factor.

The displacements of the ground and pipeline are plotted in Figure 3, where the two lines intersect at $x=L_{cros(E)}$ and $-L_{cros(E)}$. $L_{cros(E)}$ is calculated by using Equation 13, which was derived by substituting the displacement distribution function into Equation 12. Equation 13 is a nonlinear equation but can be transformed into a linear equation as represented by Equation 14, which explains that $L_{cros(E)}$ is larger than $L/4$ and the difference between the two depends on the pipe-soil interaction parameter α. A maximum longitudinal compressive strain is generated at $x=L_{cros(E)}$ and a maximum longitudinal tensile strain occurs at $x=-L_{cros(E)}$.

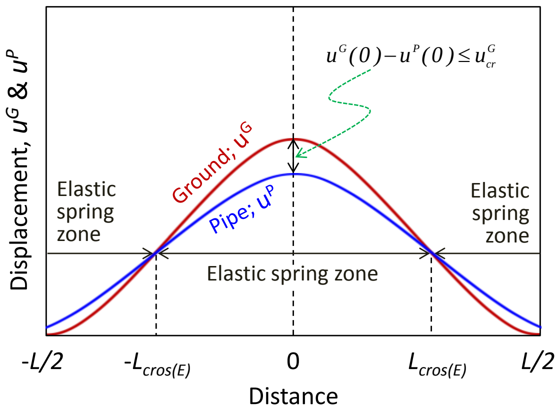

Figure 3. Displacement controlled deformation model of longitudinal slope movement

$$u^G(\pm L_{cros(E)})=u^{PE}(\pm L_{cros(E)}) \tag{12}$$

$$\cos\left(\frac{2\pi}{L}L_{cros(E)}\right)+e^{-\alpha L/2}\cosh\left(\alpha L_{cros(E)}\right)=0 \tag{13}$$

$$L_{cros(E)}=0.2466L+\frac{0.1345}{\alpha}\approx\frac{L}{4}+\frac{0.1345}{\alpha} \tag{14}$$

3.2 Solution-2: Deformation of Elastic Pipeline Constrained by Bilinear Soil Springs

When the maximum ground displacement of longitudinal slope movement increases and the soil springs tend to yield with the range $-L_{slip}\le x\le L_{slip}$, as illustrated in Figure 4, it is recognized that a pipeline deforms in the partially load controlled condition. The length of the elastic soil spring zone

L_{elas} is represented as L_{cros}-L_{slip}.

Equations 15, 16, and 17 are the complementary expressions of Equations 6, 10, and 11, respectively. Equation 15 expresses the fact that the relative displacement at $x=0$ is larger than the critical displacement of the soil springs u^G_{cr}. Therefore, Equation 16 or 17 is used to distinguish the load controlled condition from the displacement controlled condition. In cases where αL, u^G_{cr}, u^G_{max}, $u^G_{elastic}$ and F_s satisfy Equations 16 and 17, the soil springs remain elastic with the ranges $-L_{cros} \leq x \leq -L_{slip}$ and $L_{slip} \leq x \leq L_{cros}$ and yield over the range $-L_{slip} \leq x \leq L_{slip}$, as shown in Figure 4.

$$u^G_{cr} \leq u^G(0) - u^{PE}(0) \tag{15}$$

$$\frac{\alpha L}{2\pi} \leq \left\{ \left(1+e^{-\alpha L/2}\right) \frac{u^G_{max}}{2u^G_{cr}} - 1 \right\}^{1/2} \tag{16}$$

$$\frac{2u^G_{cr}}{(1-F_s)\left(1+e^{-\alpha L/2}\right)} = u^G_{elastic} \leq u^G_{max} \tag{17}$$

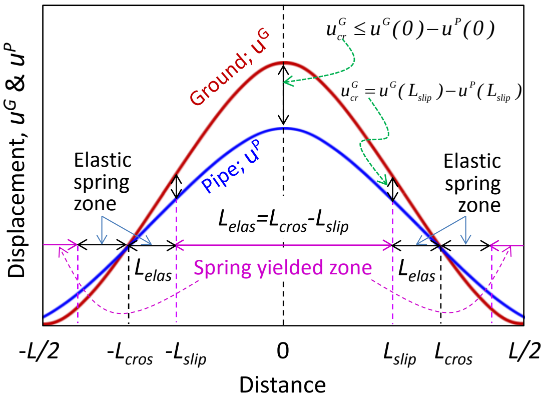

Figure 4. Partially load controlled deformation model of longitudinal slope movement

In order to derive Solution-2, it is necessary to calculate L_{cros} first by Equation 13. However, it is obvious that Equation 13 is independent of the maximum ground displacement u^G_{max}, and L_{cros} is always equal to $L_{cros(E)}$. Actually, as it is recognized that L_{cros} tends to increase with increasing u^G_{max}, any amount of attentive effort to derive an analytical solution would be in vain (Suzuki 1995). The most practical way to improve the elastic solution of Solution-2 is to consider the results of FEA.

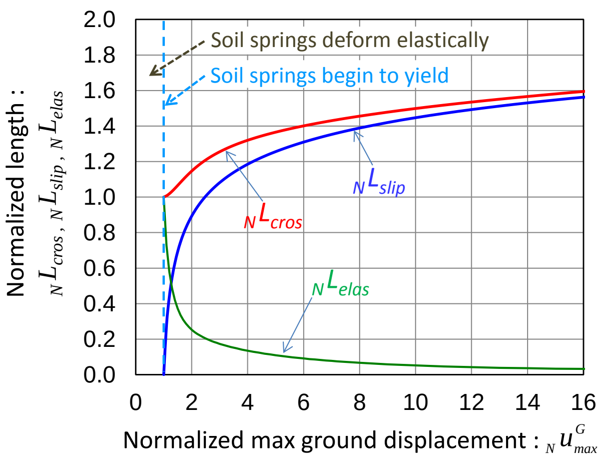

Figure 5. Variations of $_NL_{cros}$, $_NL_{slip}$ and $_NL_{elas}$ with respect to $_Nu^G_{max}$

The normalized lengths ${}_NL_{cros}$ (=$L_{cros}/L_{cros(E)}$), ${}_NL_{slip}$ (=$L_{slip}/L_{cros(E)}$) and ${}_NL_{elas}$ (=${}_NL_{cros}$-${}_NL_{slip}$) obtained by FEA are represented in terms of the normalized maximum ground displacement ${}_Nu^{Gmax}$ (=$u^G{}_{max}/u^G{}_{elastic}$) in Figure 5 (Suzuki 1995 and 2014). The regression formulas expressing ${}_NL_{cros}$ and ${}_NL_{slip}$ were obtained as Equations 18 and 19, respectively. It is clearly recognized in Figure 5 that ${}_NL_{slip}$ increases quickly and approaches ${}_NL_{cros}$ as ${}_Nu^G{}_{max}$ increases. In other words, ${}_NL_{elas}$ suddenly drops immediately after the occurrence of the slip zone and tends to be small and stable when ${}_Nu^G{}_{max}$ exceeds 6.0.

$${}_NL_{cros} = \frac{0.7292\left({}_Nu^G_{max}\right)^2 + 0.1532\left({}_Nu^G_{max}\right)}{3.043\left({}_Nu^G_{max}\right)^{1.666} + 2.976} \tag{18}$$

$${}_NL_{slip} = \frac{-0.01449\left({}_Nu^G_{max}\right)^2 + 2.564\left({}_Nu^G_{max}\right)}{2.336\left({}_Nu^G_{max}\right)^{0.8317} + 0.5385} \tag{19}$$

Here, the normalized parameters ${}_NL_{cros}$, ${}_NL_{slip}$, ${}_NL_{elas}$, and ${}_Nu^G{}_{max}$ correspond to $L_{cros}/L_{cros(E)}$, $L_{slip}/L_{cros(E)}$, $L_{elas}/L_{cros(E)}$, and $u^G{}_{max}/u^G{}_{elas}$, respectively.

If we assume a maximum ground displacement $u^G{}_{max}$, it is possible to estimate L_{cros} and L_{slip} by Equations 18 and 19, respectively. Therefore, the strain distribution $\varepsilon^{PE}(x)$ with the range $-L_{slip} \le x \le L_{slip}$ of a pipeline is calculated by Equation 20 (Suzuki 1995), and the strain distributions $\varepsilon^{PE}(x)$ with the ranges $-L_{cros} \le x \le -L_{slip}$ and $-L_{cros} \le x \le -L_{slip}$ are calculated by Equations 21 and 22. In addition, Equation 23, a second order polynomial, can be used to plot the strain distributions in place of Equations 21 and 22.

$$\varepsilon^{PE}(x) = -\alpha^2 u^G_{cr} x \qquad \left(-L_{slip} \le x \le L_{slip}\right) \tag{20}$$

$$\varepsilon^{PE}(x) = -\alpha^2\left[\left\{U_R(x) - U_R(L_{slip})\right\} + u^G_{cr}L_{slip}\right] \qquad \left(-L_{cros} \le x \le -L_{slip},\ L_{slip} \le x \le L_{cros}\right) \tag{21}$$

$$U_R(x) = \left(1 - F_s\right)\left\{\sin\left(\frac{2\pi}{L}x\right) + \frac{2\pi}{\alpha L}e^{-\alpha L/2}\sinh(\alpha x)\right\}\frac{Lu^G_{max}}{4\pi} \tag{22}$$

$$\varepsilon^{PE}(x) = -\frac{\alpha^2 u^G_{cr}}{2}\left\{\frac{\left(x - L_{cros}\right)^2}{\left(L_{slip} - L_{cros}\right)} + L_{slip} + L_{cros}\right\} \qquad \left(-L_{cros} \le x \le -L_{slip},\ L_{slip} \le x \le L_{cros}\right) \tag{23}$$

3.3 Solution-3: Deformation of Elastic Pipeline Constrained by Yielded Soil Springs

In case the maximum ground displacement of longitudinal slope movement increases and the soil springs yield over the entire length of the longitudinal slope movement, L_{cros} and L_{slip} gradually increase and L_{slip} reaches L_{cros}, as shown in Figure 6.

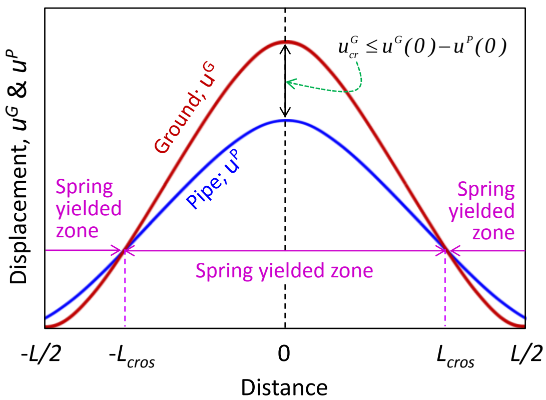

Figure 6. Load controlled deformation model of longitudinal slope movement

Figure 5 is useful to explain the variations of the normalized lengths ${}_NL_{cros}$, ${}_NL_{slip}$ and ${}_NL_{elas}$, as it represents the normalized gap between the two lines and the normalized length of the elastic spring zone. Figure 5 clarifies the fact that ${}_NL_{elas}$ tends to be smaller than 0.1 when ${}_Nu^G{}_{max}$ is larger than 6.0. In these cases, it is recognized that a pipeline deforms in the load-controlled condition.
In the case of load controlled elastic deformation, it is assumed that all the soil springs yield with the range $-L/2 \le x \le L/2$. Therefore, the strain distribution of a pipeline with the range $-L_{cros} \le x \le L_{cros}$ is represented as Equation 24. A maximum compressive strain occurs at $x=L_{cros}$, and a maximum tensile strain is generated at $x=-L_{cros}$.

$$\varepsilon^{PE}(x) = -\alpha^2 u_{cr}^G x \qquad \left(-L_{cros} \le x \le L_{cros}\right) \tag{24}$$

4. STRAIN CONVERSION PROCEDURE TO PREDICT INELASTIC PIPE STRAIN

4.1 Inelastic Longitudinal Strain of Unpressurized Pipeline

Figure 7 explains a new calculation method to estimate inelastic pipe strain by using the elastic stress or elastic strain obtained by the elastic solutions proposed in this paper. Equation 25 represents the power law relationship between the stress and the amount of plastic strain. The total stress and strain relationship is expressed as Equation 26 (Ramberg and Osgood 1943).
An elastic solution is plotted on the left in Figure 7. The inelastic pipe strain is obtained at the point where the stress-strain curve intersects the segment defined by the elastic solution and a pivot at $\varepsilon = \varepsilon_{piv}$, which is an intercept on the horizontal axis. The segment is expressed as Equation 27, where *m* and *b* are the gradient and the intercept on the vertical axis, respectively. The open rectangle represents the intercept of the stress-strain curve and the segment, and the inelastic stress and strain are the solution to be obtained.
Inserting Equation 27 into Equation 26, we obtain Equation 28, where the pipe stress σ^{PI} is the unknown parameter and the pivot strain ε_{piv} is defined as Equation 29. The inelastic pipe strain ε^{PI} can be estimated by inserting σ^{PI} into Equation 30. Finally, it is necessary to check whether ε^{PI} is an appropriate solution by comparing the ground strain ε^G. If ε^{PI} is smaller than ε^G, ε^{PI} can be adopted as the solution; otherwise, ε^{PI} is replaced with ε^G on the grounds that the pipe strain does not exceed the ground strain. The former and latter cases are shown schematically on the left and right in Figure 7, respectively. The final step of the strain conversion procedure is expressed as Equation 31.

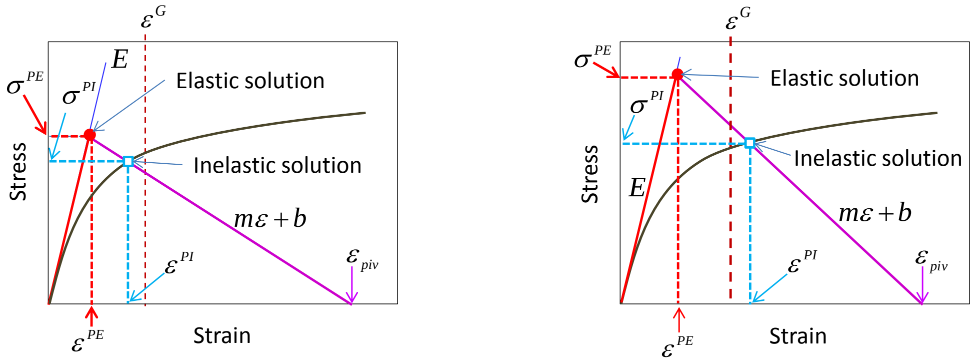

Figure 7. Calculation method of inelastic pipe strain of unpressurized pipe

$$\sigma = K\varepsilon_p^n \tag{25}$$

$$\varepsilon = \frac{\sigma}{E} + \varepsilon_{p0}\left(\frac{\sigma}{\sigma_0}\right)^N \tag{26}$$

$$\sigma = m\varepsilon + b \tag{27}$$

$$\varepsilon^{PE} = \frac{\sigma^{PI}}{E} + \frac{\varepsilon^{PE}}{\varepsilon_{piv}} \varepsilon_{p0} \left(\frac{\sigma^{PI}}{\sigma_0} \right)^N \tag{28}$$

$$\varepsilon_{piv} = \frac{u^G_{max}}{u^G_{elastic}} \varepsilon^G_{max} = \frac{\left(u^G_{max}\right)^2}{u^G_{elastic}} \frac{\pi}{L} \tag{29}$$

$$\varepsilon^{PI} = \frac{\sigma^{PI}}{E} + \varepsilon_{p0} \left(\frac{\sigma^{PI}}{\sigma_0} \right)^N \tag{30}$$

$$\varepsilon^{PI} = sign[\,\varepsilon^{PI}\,]\, min[\left|\varepsilon^{PI}\right|, \left|\varepsilon^{G}\right|] \tag{31}$$

Where, m and b are the gradient and the intercept on the vertical axis of the segment, respectively, and ε_{p0} is represented as $\varepsilon_{p0}=\varepsilon_0-\sigma_0/E$, ε_{piv} is the pivot strain, n is the strain hardening exponent, and $N=1/n$.

4.2 Inelastic Longitudinal Strain of Pressurized Pipeline

The red line in Figure 8 represents the elastic deformation of an unpressurized pipe as calculated in accordance with an appropriate elastic solution. The segment is defined between the elastic solution and the pivot strain ε_{piv}. The stress-strain curves shown in green and blue represent the axial deformation of a pressurized pipe subjected to axial compression and tension, respectively. The inelastic pipe strain will be found as the strain at the point of intersection of the segment and the stress-strain curve.

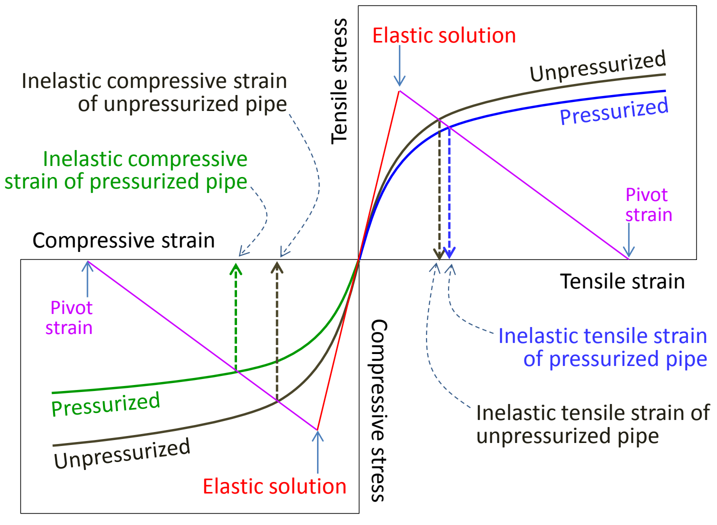

Figure 8. Calculation method of inelastic pipe strain of pressurized pipe

5. VALIDATION OF PROPOSED CALCULATION METHOD

5.1 Pipe Dimensions, Pipe Grade, Tensile Properties, and Pressure

An X65, 24" pipeline was taken as the validation model. As the thickness was assumed to be 10.2 mm, the diameter to thickness ratio D/t was 59.8. The pipeline was unpressurized or pressurized to 60% SMYS. The stress-strain curves representing the compressive and tensile deformations of the unpressurized pipes are represented in Figure 9, where the yield strength σ_0 of 450.0 MPa and the strain hardening exponent n of 0.05 were employed.

The stress-strain curves of the pressurized pipes were obtained by FEA and are also expressed in

Figure 9. As shown in the figure, the stress-strain curve for the tensile deformation of the pressurized pipe is almost the same as that of the unpressurized pipe. On the other hand, the stress-strain curve expressing compressive deformation tends to be smaller than that of the unpressurized pipe. In this case, the yield strength σ_0 and strain hardening exponent n became 343.1 MPa and 0.0684, respectively.

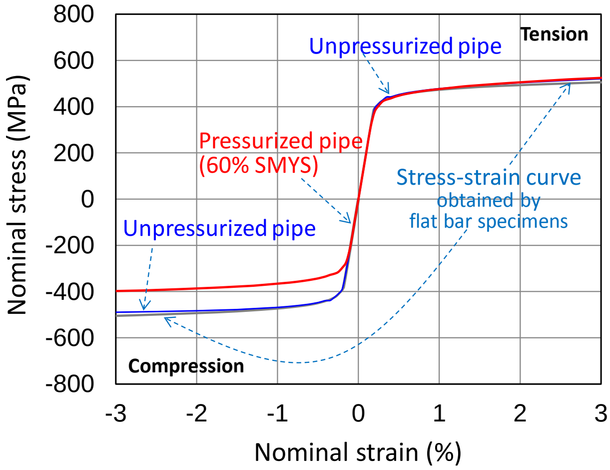

Figure 9. Stress-strain curves of X65 grade pipe

5.2 Slope Movement and Longitudinal Soil Springs

The slope movement is illustrated in Figure 10, and the ground displacement is represented by Equation 1. It was assumed that the length of the sliding zone is 100 m and the maximum displacement of the ground increases up to 100 cm. The elastic soil spring constant per unit area k of 0.0981MPa/cm and the yield displacement $u^G{}_{cr}$ of 3.0 cm were employed. Therefore, the maximum friction force per unit area becomes 0.294 MPa. Boundary elements having a semi-infinite length (Suzuki 1995) were attached at both ends of the pipeline.

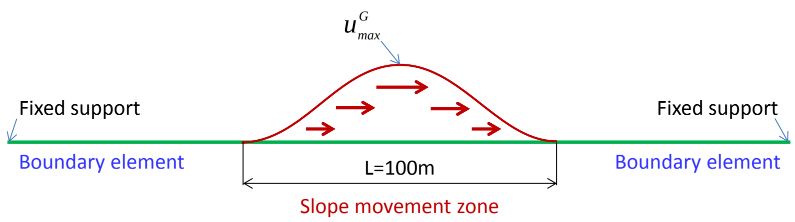

Figure 10. Ground movement at slope and X65, 24” pipeline used for validation

5.3 Strain Distribution of 24” Pipeline Calculated by Solution-1

Here we will discuss the deformation of the 24” unpressurized pipeline taking into account the maximum ground displacement $u^G{}_{max}$ of 10 cm. In this case, αL satisfies Equation 9, and Equation 10 gives ground displacement $u^G{}_{elastic}$ of 12.8 cm, which is larger than 10 cm. Hence, it is possible to use Solution-1, as the 24” pipeline deforms in the displacement controlled condition. The results in terms of the elastic pipe strain estimated by Solution-1 are plotted in Figure 11 by the open circles, which fall precisely on the pipe strain obtained by FEA.

5.4 Strain Distribution of 24” Pipeline Calculated by Solution-2

In the case that $u^G{}_{max}$ increases to 25 cm, αL satisfies Equation 16, and ${}_Nu^G{}_{max}$ and ${}_NL_{elas}$ become 1.95 and 0.26, respectively. Since these results show that the pipeline deforms in the partially load controlled condition, Solution-2 is employed for the calculation. In this case, $L_{cros(E)}$ of 26.7 m yielded L_{cros} of 30.4 m and L_{slip} of 23.2 m in the calculations by Equations 18 and 19, respectively. The strain distributions of the 24" unpressurized pipeline calculated by Solution-2 are plotted in Figure 12 over the range $-L_{cros} \leq x \leq L_{cros}$, and the results obtained by FEA are also shown for comparison.

As shown in the figure, the elastic strain distribution calculated by Solution-2 displays excellent agreement with that obtained by FEA assuming the pipeline is elastic. The inelastic pipe strain distribution was obtained in accordance with the proposed calculation method by using the cross line. The inelastic strain distribution of the pipeline also shows good agreement with the results obtained by FEA taking into account the strain hardening properties. It should be mentioned that the inelastic pipe strain becomes the same as the ground strain with the ranges $-30m \leq x \leq -25m$ and $25m \leq x \leq 30m$.

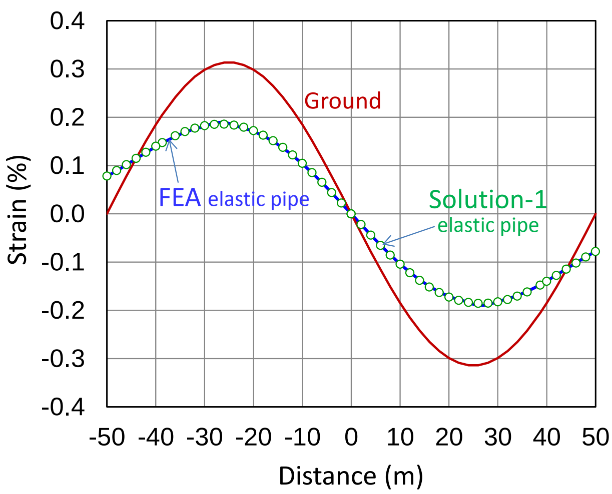

Figure 11. Strain distribution of X65, 24" unpressurized pipeline ($u^G_{max}=10cm$)

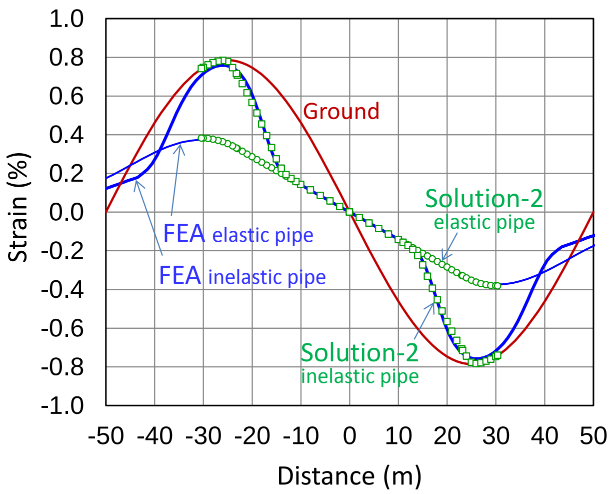

Figure 12. Strain distribution of X65, 24" unpressurized pipeline ($u^G_{max}=25cm$)

5.5 Strain Distributions of 24" Pipeline Calculated by Solution-3

In case the maximum ground displacement u^G_{max} develops to 100 cm, $_Nu^G_{max}$ and $_NL_{elas}$ become 8.71 and 0.069, respectively. Then L_{cros} of 38.7 m and L_{slip} of 36.9 m were obtained by Equations 18 and 19, respectively. Therefore, Solution-3 is applied to calculate the strain distribution of the pipeline. Figures 13 and 14 plot the strain distributions of the 24" unpressurized and pressurized pipelines, respectively. The elastic and inelastic strain distributions obtained by FEA are represented by the

thinner and thicker solid lines, respectively. The open circles express the elastic strain distribution calculated by Solution-3, and the open rectangles plot the inelastic strain distribution converted from the elastic strain distribution by using the proposed strain conversion procedure.
As shown in Figure 13, both the elastic and inelastic strain distributions of the 24" unpressurized pipeline estimated by Solution-3 coincide extremely closely with those obtained by FEA. The strain distributions of the 24" pressurized pipeline shown in Figure 14 represent almost the same tendencies as those in Figure 13.

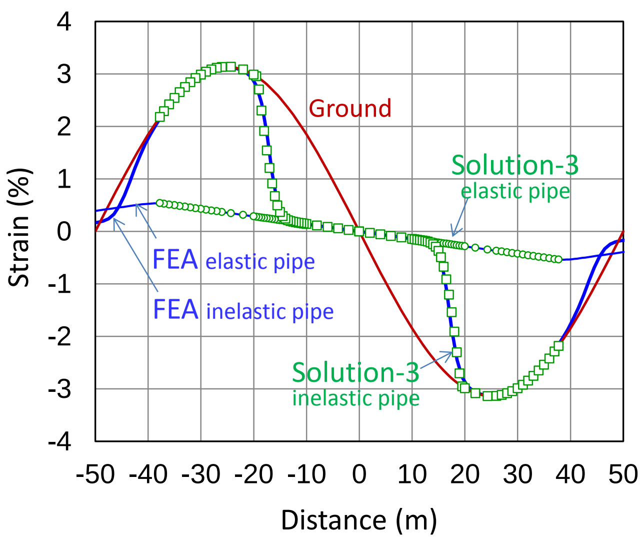

Figure 13. Strain distribution of X65, 24" unpressurized pipeline (u^G_{max}=*100cm*)

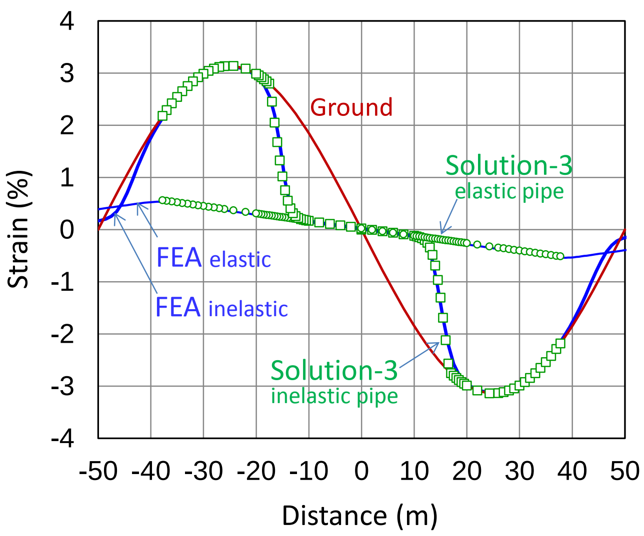

Figure 14. Strain distribution of X65, 24" pressurized pipeline (u^G_{max}=*100cm*)

6. CONCLUSIONS

A new design method to predict the inelastic strain distributions of pipelines induced by ground movement was proposed by adopting the elastic solutions and strain conversion procedure. Consequently, the proposed design method was validated by comparing the strain distributions obtained by FEA. The results are summarized as follows.

- The elastic strain distributions of the unpressurized pipeline estimated by the elastic solutions showed excellent agreement with the results obtained by FEA.

- The inelastic strain distributions of the unpressurized and pressurized pipelines predicted by Solution-2 or Solution-3 were also in good agreement with the results calculated by FEA.
- The strain conversion procedure was found to be appropriate for predicting the inelastic strain distribution of a pipeline under both unpressurized and pressurized conditions.
- The pivot strain is the key parameter for the strain conversion procedure, which pivot strain depends on the profile of the slope movement and the pipe-soil interaction parameter.
- The proposed design method makes it possible to investigate the effects of tensile properties or strain hardening properties on the magnitude of inelastic pipe strain.

7. ACKNOWLEDGMENTS

The authors wish to thank JFE Steel Corporation for permission to publish this paper. The contribution made by Izumi Kubo of the Japan Industrial Testing Corporation in preparing this paper was greatly appreciated.

8. REFERENCES

ASCE (1984). Guidelines for the seismic design of oil and gas pipeline systems, *Committee on Gas and Liquid Fuel Lifelines*, TECLEE, American Society of Civil Engineers.

JGA (2001). Seismic design guideline of high pressure gas pipeline to withstand liquefaction-induced permanent ground deformation, *JGA (Seismic Design Guideline)-207-01*, Japan Gas Association. (Japanese)

JGA (2016). Seismic design guideline of high pressure gas pipeline to withstand liquefaction-induced permanent ground deformation, *JGA (Guideline)-207-01*, Japan Gas Association. (Japanese)

JGA (1983). Seismic design guideline of high pressure gas pipeline, *JGA (Seismic Design Guideline)-206-03*, Japan Gas Association. (Japanese)

JGA (2004). Seismic design guideline of high pressure gas pipeline, *JGA (Seismic Design Guideline)-206-03*, Japan Gas Association. (Japanese)

Kuesel TR (1969). Earthquake design criteria for subways, *Journal of the Structure Division*, ASCE, Vol. 95, No. ST6.

Ramberg W, Osgood WR (1943). Description of stress-strain curve by three parameters, *Technical Note of National Advisory Committee for Aeronautics*, NACA-TN-902.

Suzuki N, Nakane H (1989). Idealization of liquefaction-induced permanent ground deformation for seismic design of pipeline, *Journal of Structural Engineering*, Vol. 36A, 1365-1376, JSCE. (Japanese)

Suzuki N (1995). Pipeline design to withstand liquefaction-induced permanent ground deformation, *Ph.D. Thesis*, Tohoku University. (Japanese)

Suzuki N (2014). An overview of strain-based seismic design of high pressure gas pipeline, *Journal of Pipeline Engineering*, 3rd Quarter, 211-222.